

# Crystallization behavior of some melt spun Nd-Fe-B alloys

M.T. Clavaguera-Mora, M. D. Baró, and S. Suriñach

*Física de Materials, Dept. Física, Universitat Autònoma de Barcelona, 08193-Bellaterra, Spain*

N. Clavaguera

*Dept. Estructura i Constituents de la Matèria, Facultat de Física, Diagonal 647, 08028-Barcelona, Spain*

(Received 2 February 1990; accepted 19 February 1990)

The kinetics of crystallization of four amorphous (or partially amorphous) melt spun Nd-Fe-B alloys induced by thermal treatment is studied by means of differential scanning calorimetry and scanning electron microscopy. In the range of temperatures explored experimentally, the crystallization process is thermally activated and generally proceeds in various stages. The Curie temperature and the crystallization behavior have been measured. The apparent activation energy of crystallization of most of the crystallization stages has been determined for each melt spun alloy. The explicit form of the kinetic equation that best describes the first stage of crystallization has been found. It follows in general the Johnson-Mehl-Avrami-Erofe'ev model, but clear deviations to that model occur for one alloy. Scanning electron microscopy demonstrates that preferentially heterogeneous nucleation occurs at the ribbon surface which was in contact with the wheel. From crystallization kinetics results the lower part of the experimental time-temperature-transformation curves for all studied alloys are deduced and extrapolated to the high temperature limit of their range of validity, also deduced.

## I. INTRODUCTION

The development of a rare earth iron-based permanent magnet has been a long-standing goal of the permanent magnet industry. The first successful attempts to magnetically harden these materials employed rapid solidification techniques which produced partially or totally amorphous alloys.<sup>1</sup> The aim of rapid solidification is to utilize the wide range of metastable microstructures accessible by liquid quench and subsequent heat treatment of these alloys. Consequently, the study of the changes induced by heat treatment is of great concern in every application.<sup>2-4</sup>

The purpose of the present work was the detailed measurement of the crystallization kinetics of some amorphous (or partially amorphous) melt spun Nd-Fe-B alloys. The calorimetric study was performed by differential scanning calorimetry (DSC) in both isothermal and continuous heating regimes, and the kinetic parameters of the main process were obtained. These measurements were completed with microstructural analysis carried out by scanning electron microscopy (SEM).

## II. EXPERIMENTAL

Master alloys of several compositions (see Table I) were provided by Dr. S. Sattelberger from Gesellschaft für Elektrometallurgie, Nürnberg. From these materials, melt spun samples were obtained by quenching the

molten alloys on the surface of a rapidly spinning (~30 m/s) copper wheel under a helium atmosphere. Melt spun alloys #1, #2, and #3 were obtained as a mixture of short ribbons and flakes, and their x-ray diffraction patterns showed a small degree of crystallinity on them (~10 vol%). Melt spun alloy #4 was obtained in normal ribbon form, and x-ray diffraction confirmed its amorphous state within the limit of detection of crystals.

Calorimetric measurements were performed in a Perkin-Elmer DSC-2 on 5-15 mg of material under pure argon atmosphere. Isothermal anneals were performed in the DSC by heating from room temperature at a rate of 320 K/min to the annealing temperature. The experiments at constant heating rate were recorded from room temperature to temperatures above the crystallization exotherms at scanning rates ranging from 10 to 320 K/min. No oxidation of the material was observed after these treatments. The crystallization process has been studied in the range 800-960 K. The fraction of crystallized material,  $x$ , at a given time,  $t$ , was determined from the ratio between the subtended area at that time and the area of the complete exothermic peak. Similarly, the transformation rate,  $dx/dt$ , at the time,  $t$ , was determined by the ratio between the height of the DSC curve at that time and the complete area. The error estimated for  $dx/dt$  in the range  $0.1 \leq x \leq 0.9$  is less than 5%. The calibration procedure is described elsewhere.<sup>5</sup> Microstructural observations on fresh fracture surfaces were made with a SEM Hitachi S-570.

TABLE I. Composition, Curie temperature,  $T_C$ , and beginning of crystallization  $T_X$  (at a scan rate of 40 K/min) of the melt spun alloys studied.

Alloy	Composition	$T_C$ (K)	$T_X$ (K)
#1	Nd <sub>13</sub> Fe <sub>82.2</sub> B <sub>4.8</sub>	575	845
#2	Nd <sub>13</sub> Fe <sub>79</sub> B <sub>8</sub>	579	857
#3	Nd <sub>8.5</sub> Fe <sub>80.5</sub> B <sub>11</sub>	648	870
#4	Nd <sub>3</sub> Fe <sub>77</sub> B <sub>20</sub>	577 <sup>a</sup> 765	833

<sup>a</sup>Amorphous

### III. RESULTS AND DISCUSSION

#### A. Calorimetric behavior

The differential scanning calorimetric behavior of the as-quenched material, including ribbons and flakes in alloys #1 to #3, was dependent on the relative amount of flakes. This is so because most probably the degree of crystallinity of the short ribbons obtained is different from that of the flakes. But the reproducibility on DSC results was good when the flakes were analyzed alone. Therefore, only flakes of alloys #1 to #3 were used in the calorimetric analysis. No such problem appeared for alloy #4.

The DSC scans at a heating rate of 40 K/min are shown in Fig. 1 for the four melt spun alloys studied. On heating the Curie transition is observed, except for alloy #3. The values of both the Curie temperature,  $T_C$ , and the beginning of crystallization,  $T_X$ , are shown in

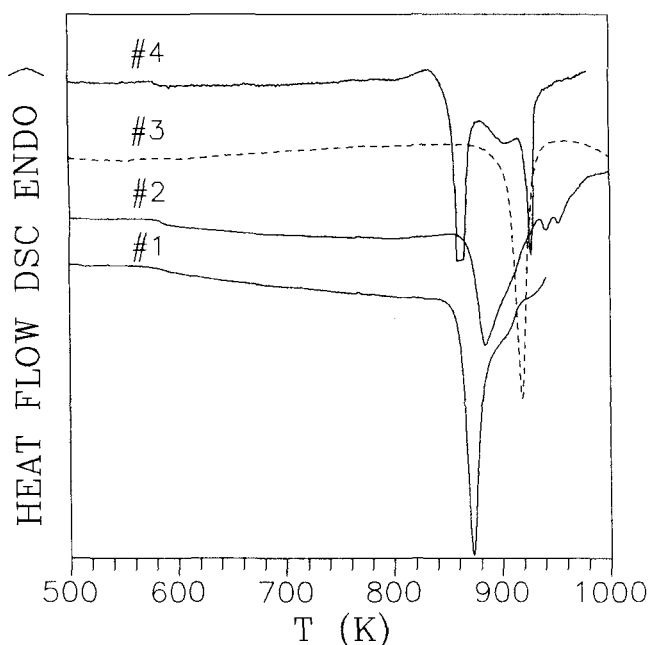


FIG. 1. DSC scans for the four melt spun alloys studied (scan rate 40 K/min).

Table I. The Curie temperature of both the melt spun and the recrystallized material has the same value for alloys #1 and #2, but the specific heat anomaly is much smaller for the melt spun material, indicating that the transition observed in the melt spun material is that of its crystalline part. For alloy #3 the value quoted in Table I is that of the crystallized material. In alloy #4 it was possible to observe the Curie temperature of both the amorphous phase and the crystallized material; the glass transition could also be observed for this alloy, and it occurs at a temperature  $T_g = 803$  K.

According to Ref. 6, the crystallization product in alloys #1 and #2 is off-stoichiometric Nd<sub>2</sub>Fe<sub>14</sub>B whereas the crystallization products of alloys #3 and #4 are, respectively, Nd<sub>2</sub>Fe<sub>23</sub>B<sub>3</sub>, Fe and Fe<sub>3</sub>B, Nd<sub>2</sub>Fe<sub>14</sub>B (very small amount). Our results on  $T_C$  are in agreement with these findings.<sup>6,7</sup>

As seen in Fig. 1, crystallization occurs in one or in various steps which appear as overlapped peaks in the DSC curves. The general form of the exothermic peaks agrees with that published for melt spun alloys of similar composition.<sup>8,9</sup>

#### B. Kinetics of crystallization

To study the crystallization kinetics we assume, as is often the case in metallic glasses, that each crystallization peak follows a kinetic equation of the form  $dx/dt = K(T)f(x)$ , which gives the rate of reaction as a function, in separate variables, of the fraction crystallized,  $x$ , and of the temperature,  $T$ . We further assume that the rate constant  $K$  follows the Arrhenius behavior  $K(T) = K_0 \exp(-E/RT)$  with  $E$  the apparent activation energy and  $K_0$  the pre-exponential factor. The apparent activation energy for the main peaks was deduced from the Kissinger plot of  $\ln(r/T^2)$  vs  $1/T$  with  $r$  the heating rate and  $T$  the temperature of the maximum of the peak.<sup>10</sup> The values obtained are presented in Table II.

An accurate kinetic treatment of all the peaks was hindered by their overlapping. However, isothermal

TABLE II. Crystallization data of the melt spun alloys.

Alloy	Peak	$E$ (eV)	$g(x = 0.1)/K_0$ (s)	$T_{max}$ (K)
#1	First	2.99	$1.4 \times 10^{-16}$	930
#2	First	3.21	$8.9 \times 10^{-18}$	860
	Second	3.65		
	Third	4.73		
	Fourth	5.18		
#3	First	4.54	$1.1 \times 10^{-24}$	840
#4	First	5.91	$2.9 \times 10^{-34}$	870
	Third	3.95		

measurements on each alloy enabled us to obtain, except for a constant factor, the value of  $f(x)$  for the first crystallization peak. This is so because the general kinetic equation can be rewritten in logarithmic form as  $\ln(dx/dt) = \ln[K_0 f(x)] - E/RT$ .

The dependence of  $\ln[K_0 f(x)]$  on  $\ln(1-x)$ , obtained from the isotherms, is shown in Figs. 2 to 5 for each alloy. The points represent the experimental results and the full lines, the values calculated by use of

the Johnson-Mehl-Avrami-Erofe'ev (JMAE) model for  $f(x)$ , namely  $f(x) = n(1-x)[-\ln(1-x)]^{(n-1)/n}$ . There is good agreement between the experimental points and the values predicted by this model with  $n = 3.3$  for alloy #3. The agreement is less good for alloys #1 and #2, the best fit being obtained for  $n = 2.3$  and 2.0, respectively. For alloy #4 neither this model nor any other of the current models used in kinetics of transformation studies<sup>5</sup> is able to reproduce the results.

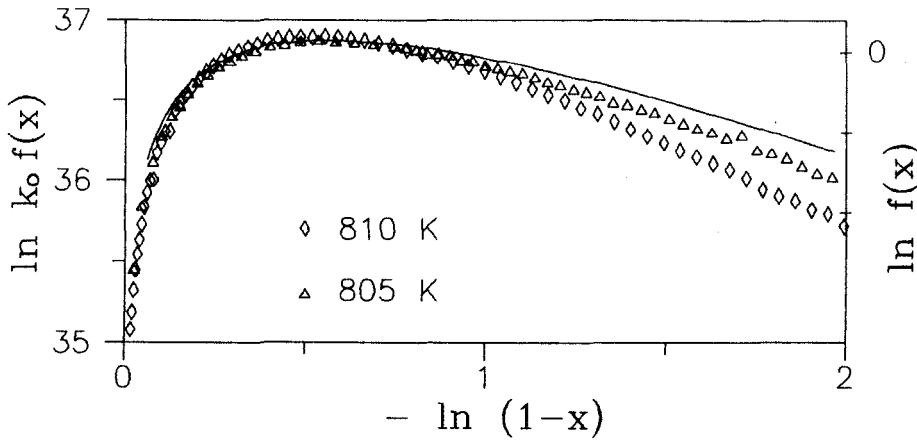


FIG. 2.  $\ln[K_0 f(x)]$  vs  $-\ln(1-x)$  for alloy #1. Experimental data at 805 and 810 K are shown along with the best theoretical curve for  $f(x)$  (JMAE model with  $n = 2.3$ ).

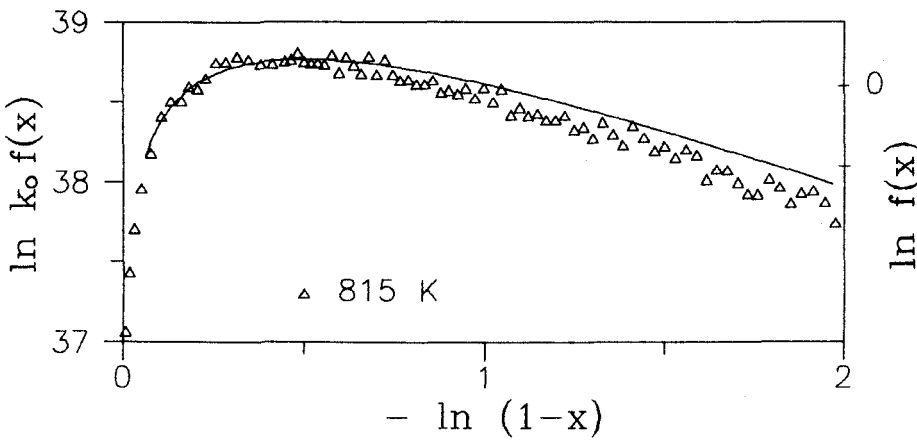


FIG. 3.  $\ln[K_0 f(x)]$  vs  $-\ln(1-x)$  for alloy #2. Experimental data at 815 K are shown along with the best theoretical curve for  $f(x)$  (JMAE model with  $n = 2.0$ ).

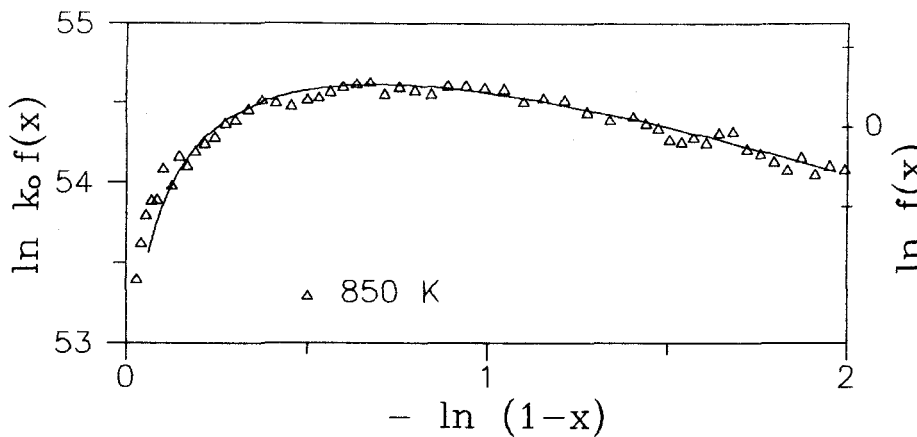


FIG. 4.  $\ln[K_0 f(x)]$  vs  $-\ln(1-x)$  for alloy #3. Experimental data at 850 K are shown along with the best theoretical curve for  $f(x)$  (JMAE model with  $n = 3.3$ ).

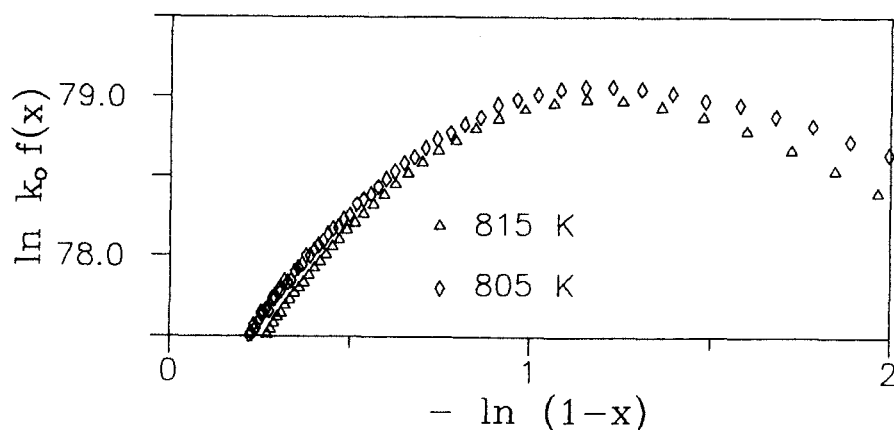


FIG. 5.  $\ln[K_0 f(x)]$  vs  $-\ln(1-x)$  for alloy #4. Experimental data at 805 and 815 K.

### C. SEM analysis

Some fresh fractures of the melt spun ribbons before and after heat treatment were observed by SEM. This examination showed that crystallization begins very often on the surface that was in contact with the wheel, and growth occurs perpendicularly to this surface. Figure 6 shows the secondary electron image of a typical fracture of a heat-treated sample. It corresponds to alloy #2 after annealing for 30 min at 815 K. A bar-shaped structure can be seen perpendicular

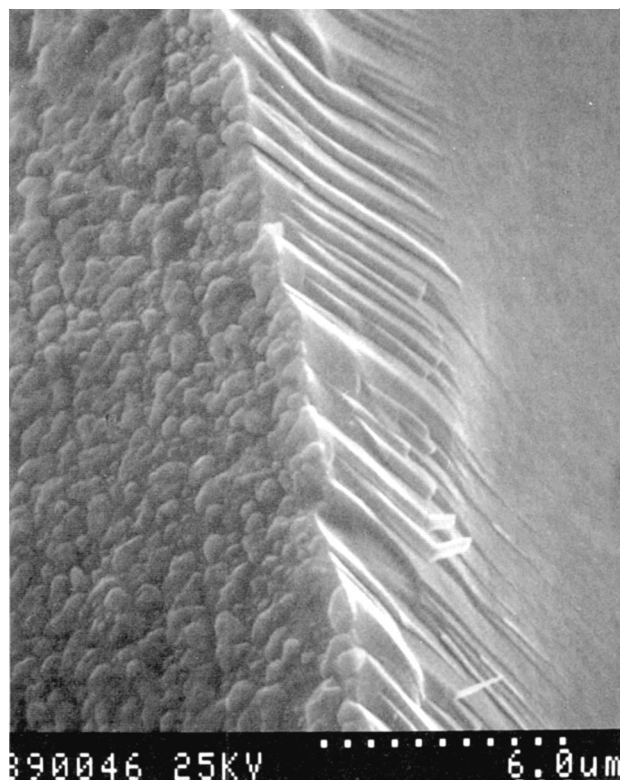


FIG. 6. Microscopic image of the fracture of alloy #2 after annealing 30 min at 815 K (scanning electron micrograph).

to the aforementioned surface, indicative of preferential growth in that direction. Further studies are in progress to determine the grain size of the heat-treated materials.

### D. Determination of the T-T-T curves

The time-temperature-transformation (T-T-T) curve can be constructed, as shown by Uhlmann<sup>11,12</sup> and Davies,<sup>13</sup> from a kinetic treatment based on classical nucleation and crystallization theories. A critical requirement of this treatment is a knowledge of the temperature dependence of the viscosity in the undercooled liquid regime between the normal melting point and the glass transition temperature, and these data are unfortunately rarely available. Another difficulty of Uhlmann's treatment arises from the fact that he assumes the occurrence of homogeneous nucleation, which is a rather unlikely event during a rapid cooling of the melt.

Now, the study of crystallization kinetics is just a part of the general determination of the T-T-T curve. Therefore, the DSC technique is very useful for determining the classical T-T-T curve.<sup>14-18</sup> Effectively, under isothermal conditions the integrated form of the kinetic equation is

$$g(x) = \int_0^x \frac{dx}{f(x)} = K(T)t \quad \text{or} \quad \frac{g(x)}{K_0} = t \exp(-E/RT) \quad (1)$$

The time needed to crystallize a certain fraction  $x$  of metallic material, at a given temperature, can be obtained by DSC when using the isothermal mode to detect the onset of crystallization, after a rapid change of temperature from the glassy state ( $T < T_g$ ) to the temperature of observation. However, the range of temperatures that can be used to detect the onset of crystallization in the isothermal mode is very limited in most metallic alloys because they tend to crystallize during the rapid temperature change monitored in the

DSC prior to observation. The most reliable method to extend the experimental determination of the T-T-T is to take advantage of the knowledge of the crystallization kinetics. That is, the plot of temperature versus the time needed at that temperature to get a fixed value of  $x$ , as deduced from Eq. (1), gives the T-T-T curve in the temperature interval for which Eq. (1) is valid. In practice,  $g(x)/K_0$  can be deduced from the results obtained in an isothermal scan, and the value of  $E$  can be obtained from continuous heating results (peak method, for instance).

In general, Eq. (1) may replace the T-T-T curve only in the temperature interval of validity of the kinetic equation. This equation is plotted in Fig. 7 together with the general form of the T-T-T curve. As seen in that figure, Eq. (1) reproduces rather well the lower part of the T-T-T curve. However, it deviates from it at temperatures near to the nose of the T-T-T curve. Using the method developed by Uhlmann<sup>11</sup> based on the classical theories of crystal nucleation and growth, the highest temperature  $T_{max}$  to which Eq. (1) can reasonably well reproduce the T-T-T curve can be estimated to be  $T_{max} \sim 0.6 T_l$ ,  $T_l$  being the liquidus temperature (see Appendix).

The values of  $g(x)/K_0$  obtained for the four alloys studied are quoted for  $x = 0.1$  in Table II (some uncertainty arises because the melt spun alloys #1 to #3 are not totally amorphous). Insofar as all the kinetic parameters are known, we can construct the T-T-T curves for the various melt spun alloys. This has been done, and the curves obtained are plotted in Fig. 8. The experimental points obtained in the isothermal regime are also shown in Fig. 8. Because of the assumptions

inherent in this approach, as explained before (mainly to take a constant value for the apparent activation energy of crystallization), we cannot extend the validity of the treatment to temperatures higher than  $T_{max}$  (presented in Table II). With that limitation, the curves plotted in Fig. 8 can be considered as good estimates of the low temperature part of the T-T-T curves. They are important because they can be used as a guide for the choice of the heat treatment needed to obtain a certain microstructure and, as a consequence, they permit magnetic performance to be optimized.<sup>19</sup>

#### IV. CONCLUSIONS

Melt spun Nd-Fe-B alloys have been prepared under controlled atmospheric conditions and their thermal behavior has been examined by DSC and SEM. Calorimetric analysis shows that crystallization proceeds generally in various stages. By systematic measurements in both isothermal and continuous heating modes, it was possible to deduce optimal estimates of some of the kinetic parameters for most of the crystallization stages. Microscopical analysis suggests that crystallization develops from the surface that was in contact with the wheel and perpendicular to it. The lower part of the T-T-T curves was also deduced for all the melt spun alloys, as it is a guide to optimize magnetic performance of heat-treated materials.

#### ACKNOWLEDGMENTS

This work was supported by EURAM [contract No. MA1E.0061.C(H)] and by CICYT (project No. MAT88-0314), which are acknowledged.

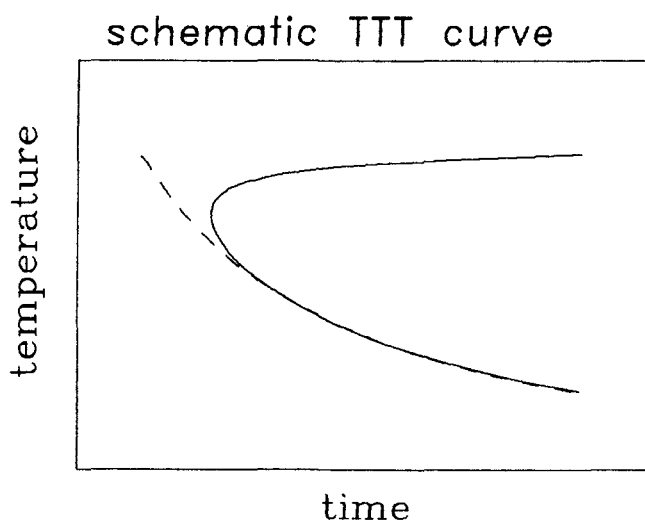


FIG. 7. Solid line represents the schematic time-temperature-transformation curve for a glass-forming alloy, and dashed line is its asymptotic behavior at low temperatures given by the equation  $t \exp(-E/RT) = \text{constant}$ .

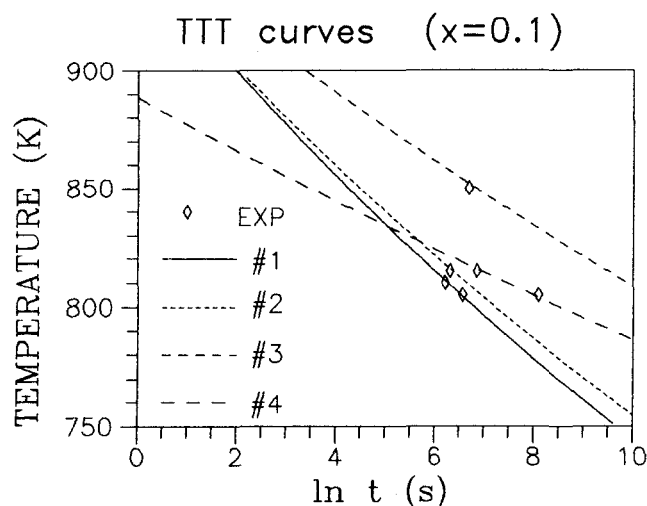


FIG. 8. Predicted low temperature part of the T-T-T curves for the four Nd-Fe-B alloys studied. Experimental points obtained from isothermal DSC scans.

## REFERENCES

- <sup>1</sup>A. E. Clark, Appl. Phys. Lett. **23**, 642 (1977).  
<sup>2</sup>K. H. J. Buschow, Mater. Sci. Rep. **1**, 1 (1986).  
<sup>3</sup>Several papers in Mater. Sci. Eng. **99**, 123-173 (1988).  
<sup>4</sup>S. Hatta and T. Mizoguchi, Jpn. J. Appl. Phys. **27**, 2078 (1988).  
<sup>5</sup>S. Suriñach, M. D. Baró, M. T. Clavaguera-Mora, and N. Clavaguera, J. Non-Cryst. Solids **58**, 209 (1983).  
<sup>6</sup>K. H. J. Buschow, D. B. de Mooij, and H. M. van Noort, J. Less-Common Met. **125**, 135 (1986).  
<sup>7</sup>K. H. J. Buschow, D. B. de Mooij, J. L. C. Daams, and H. M. van Noort, J. Less-Common Met. **115**, 357 (1986).  
<sup>8</sup>A. J. W. Ogilvy, G. P. Gregan, and H. A. Davies, in *Nd-Fe Permanent Magnets, Their Present and Future Applications*, edited by I. V. Mitchell (CEC, Brussels, 1985), p. 93.  
<sup>9</sup>A. Jha, H. A. Davies, and R. A. Buckley, J. Magn. and Magn. Mater. **80**, 109 (1989).  
<sup>10</sup>D. W. Henderson, J. Non-Cryst. Solids **30**, 301 (1979).  
<sup>11</sup>D. R. Uhlmann, in *Materials Science Research*, edited by T. J. Gray (Plenum Press, New York, 1969), Vol. 4, p. 172.  
<sup>12</sup>D. R. Uhlmann, J. Non-Cryst. Solids **7**, 337 (1972).  
<sup>13</sup>H. A. Davies, J. Non-Cryst. Solids **17**, 266 (1975).  
<sup>14</sup>N. Clavaguera, M. T. Clavaguera-Mora, and J. Casas-Vázquez, J. Non-Cryst. Solids **22**, 23 (1976).  
<sup>15</sup>P. M. Anderson, III and A. E. Lord, Jr., Mater. Sci. & Eng. **43**, 93 (1980).  
<sup>16</sup>E. A. Marseglia and E. A. Davis, J. Non-Cryst. Solids **50**, 13 (1982).  
<sup>17</sup>D. R. MacFarlane, R. K. Kadlyala, and C. A. Angell, J. Chem. Phys. **87**, 1094 (1983).  
<sup>18</sup>C. A. Angell, J. Non-Cryst. Solids **102**, 205 (1988).  
<sup>19</sup>H. A. Davies, K. J. A. Mawella, R. A. Buckley, G. E. Carr, A. Manaf, and A. Jha, in *Concerted European Action on Magnets (CEAM)*, edited by I. V. Mitchell, J. M. D. Coey, D. Givord, I. R. Harris, and R. Hanitsch (Elsevier, 1989), p. 543.

## APPENDIX

For single component materials or congruently melting compounds, neglecting transient time effects, the volume fraction  $x$  crystallized at time  $t$  may be related to the homogeneous nucleation rate  $I$  and to the crystal growth  $u$ , by

$$x = 1 - \exp[-(\pi I u^3 t^4/3)] \quad (\text{A1})$$

Considering the classical transformation kinetics, crystal nucleation and growth theory give, respectively,<sup>11</sup>

$$I = \frac{I_0}{\eta} \exp\left[-\frac{16\pi}{3} \frac{\alpha^3 \beta}{(\Delta T_r)^2 T_r^3}\right] \quad (\text{A2})$$

$$u = \frac{u_0}{\eta} [1 - \exp(-\beta \Delta T_r)] \quad (\text{A3})$$

with

$$I_0 = N_v kT/3\pi a_0^3; \quad u_0 = f kT/3\pi a_0^2 \quad (\text{A4})$$

$$\eta = \eta_0 \exp[a/(T - T_0)] \quad (\text{A5})$$

$$\alpha = \sigma/\Delta H_m; \quad \beta = \Delta H_m/RT_m \quad (\text{A6})$$

$$T_r = T/T_m; \quad \Delta T_r = 1 - T_r \quad (\text{A7})$$

Here  $N_v$  is the mean volume concentration of atoms,  $a_0$  is the atomic diameter,  $\eta$  is the viscosity,  $\sigma$  is the molar free interface enthalpy between nucleus and liquid,  $T_m$  and  $\Delta H_m$  are the temperature and molar enthalpy of fusion, respectively, and  $f$  is the fraction of sites at the crystal-liquid interface where atoms may preferentially be added and removed.

The nose of the T-T-T curve is obtained from Eq. (A1) by the condition

$$(dt/dT)_{x=\text{const}} = 0 \quad (\text{A8})$$

This condition may be rewritten as

$$d[\ln(I)]/dT + 3d[\ln(u)]/dT = 0 \quad (\text{A9})$$

Employing Eqs. (A2) to (A7), this condition transforms to

$$\frac{4a}{(T - T_0)^2} + \frac{3}{T_m T_r \Delta T_r} + \frac{16\pi}{3} \frac{\alpha \beta^3}{T_r^4 (\Delta T_r)^3 T_m} (3 - 5T_r) = 0 \quad (\text{A10})$$

As  $a$ ,  $T_r$ ,  $\Delta T_r$ ,  $\alpha$ ,  $\beta$ , and  $T_m$  all have positive values, the nose of the T-T-T curve occurs for  $T_r > 3/5$ . But the maximum value of  $T_r$  is one. Therefore, we can estimate the temperature of the nose of the T-T-T curve as occurring for  $T_r \sim 4/5$ . In general, for alloys of any composition the estimate will generalize to  $T \sim 0.8 T_l$ , where  $T_l$  is the liquidus temperature. To be safe, the limit of validity of the asymptotic behavior determined by crystallization kinetic studies can be estimated as  $T_{\text{max}} \sim 0.6 T_l$ .